

Research Article

Research on Dynamic Evaluation Model of Slope Risk Based on Improved VW-UM

Haiping Xiao ^{1,2}, Guangli Guo ¹, and Lanlan Chen³

¹NASG Key Laboratory of Land Environment and Disaster Monitoring, China University of Mining and Technology, Xuzhou, China

²School of Architectural and Surveying Engineering, Jiangxi University of Science and Technology, Ganzhou, China

³College of Applied Sciences, Jiangxi University of Science and Technology, Ganzhou, China

Correspondence should be addressed to Guangli Guo; pro_guogl@163.com

Received 25 September 2018; Revised 10 December 2018; Accepted 18 December 2018; Published 6 February 2019

Academic Editor: Enrico Conte

Copyright © 2019 Haiping Xiao et al. This is an open access article distributed under the Creative Commons Attribution License, which permits unrestricted use, distribution, and reproduction in any medium, provided the original work is properly cited.

There are many accidents of slope failure due to rainfall at home and abroad, which have caused heavy casualties and property losses. Stability analysis and evaluation of slope have become a research hotspot. Aiming at the slope stability under different rainfall, this paper takes Yuebao Open-pit Mine slope as an example, has constructed a dynamic variable weight (VW) model of influencing factors on slope stability, and has analyzed the dynamic change and correlation of the slope indexes weights under different monthly maximum rainfall. On this basis, the dynamic evaluation model of slope stability has been established based on uncertainty measurement (UM), and the risk importance (RI) q which is proposed has quantitatively evaluated the risk degree of slope. The results show that under different monthly maximum rainfall the weight of each index is no longer a fixed value but a nonlinear and dynamic change law, and there is a strong correlation among the monthly maximum rainfall, internal friction angle, and cohesion. In addition, the q increases gradually with the increase of the monthly maximum rainfall, and the stability evaluation results are highly consistent with the HPI slope, which have verified the reliability of the dynamic evaluation model. So, it can provide technical support for the safety production and management of open-pit slope and can also provide reference for related research.

1. Introduction

With the continuous expansion of the scale and depth of open-pit mine, the slope of the mine becomes steeper and higher gradually, and the high and steep slope is formed. However, many safety hazards are derived, leading to slope collapse, landslides, and other serious geological disasters due to the influence of geological conditions and external environment. According to the references [1–9], the slope failure at home and abroad is mostly related to rainfall, accounting for about 90% of the total number of landslides, which has caused significant casualties and property losses. Table 1 lists the landslide accidents affected by rainfall in some mining areas in recent five years. Therefore, the stability analysis and landslide prediction of open-pit slope under rainfall conditions provide important decision-making basis for disaster prevention, disaster reduction, and disaster relief, which have great practical significance and far-reaching

social significance for social stability and ecological environment protection.

In the past few decades, many scholars at home and abroad have carried out remarkable researches on landslide stability analysis and disaster warning caused by rainfall, which have achieved fruitful results. Ji et al. [10] had established a mathematical model of landslide safety factor, rainfall intensity and rainfall duration through rainfall model test and laboratory test, and verified the reliability of the fitting equation. Lin et al. [11] had used the physical model method to study the damage process and characteristics of rainfall on oblique and inclined slopes and revealed the influence mechanism of rainfall intensity on landslide. Li et al. [12] had used the semisimilar material physical model test method to analyze the starting conditions and sliding mechanism of loess-mudstone interface landslide under different rainfall conditions. Li et al. [13] had carried out a model test of indoor slope landslide by self-developed model test device

TABLE 1: Landslide accidents in some mining areas in the recent 5 years in China.

Time	Landslide location	Rainfall conditions	Accident situation
April 26, 2012	Quarry of Pinggui Management Area	Continuous heavy rainfall	Four dead
August 4, 2012	Nanfen Open-pit Mine	Daily rainfall reached 215.4 mm	A large range of mass landslides
April 3, 2014	Quarry of Fenyi County Qishan Stone Industry Co., Ltd.	Continuous rainfall for several days	Three dead
May 22, 2014	JinlongSheying Porcelain Clay Mine in Heyuan city	Continuous multiday rainstorm	Six dead and one wounded seriously
August 3, 2015	Original Open-pit Mine of Inner Mongolia Aohan Banner Baota Oil Shale Company	Persistent rainstorm	Six buried
August 11, 2017	Shanxi HeshunLvxin Coal Mining Area	Continuous heavy rainfall	Nine dead and one wounded

and analyzed the characteristics of slope landslide under the action of previous rainfall. Dong et al. [14] had studied the stability of gravel soil slope by means of indoor artificial heavy rainfall. Suradi et al. [15] had used indoor experiments and numerical simulation methods to study and analyze the landslide caused by extreme rainfall in northern Australia. Lo et al. [16] had obtained the relevant calculation parameters based on the image and field survey data and analyzed the landslide trend and mechanism of the slope under rainfall induced state by numerical simulation. He et al. [17] had quantitatively studied the influence of rainfall on the stability of the dump slope and established a numerical model of seepage flow in the dump, which shows that the rainfall greatly reduces the safety factor of the slope stability. Zhao et al. [18] had used Geostudio software to analyze and study the stability of rock slope under rainfall and blasting vibration conditions, which shows that groundwater has a very obvious influence on the stability of rock slope. Yang et al. [19] had used SEEP/W finite element software to simulate the whole process of seepage field change of slope rock mass under the condition of heavy rainfall infiltration and calculated the slope stability coefficient and slope stress and strain at different seepage moments. Li et al. [20] had used ABAQUS software to solve the maximum displacement and safety factor of the slope and considered the stability of the slope based on the boundary conditions of rainfall infiltration. Saadatkhah et al. [21, 22] had used the TRIGRS model to simulate the spatiotemporal regions of slope damage induced by rainfall in the Hulu-Krone region of Malaysia. Mao et al. [23] had used the uncertainty factor rainfall induced by landslide as the research object and introduced the uncertain support vector machine algorithm to establish a landslide hazard prediction model. Shen et al. [24] had used the two-level fuzzy comprehensive evaluation method to analyze the slope stability based on the influence of rainfall on the weight of each influencing factor, which are consistent with the classical limit equilibrium method and consistent with the field investigation. Although the above research results have an important role in promoting the mechanism of rainfall induced landslide, slope stability and disaster warning, some results ignore the weight of the influencing factors in the landslide (importance) and the indicators under different rainfall conditions, and some results neglect the degree of correlation between influencing factors, which leads to unclear research about the correlation between the influence factors and slope stability.

In view of the shortcomings of the above references and related research results and taking into account the complexity and uncertainty of the slope stability, it is difficult to describe the change with the exact quantitative method. So, it cannot well realize the analysis of dynamic change and correlation degree of the slope influencing factors and the quantitative evaluation of the slope risk degree. But at present, in resolving uncertain information or data, researchers at home and abroad have used the unascertained measurement evaluation model with special advantages for natural and social sciences such as goaf stability evaluation [25], landslide risk evaluation of dump [26], highway traffic efficiency evaluation [27], underground mining method selection [28],



FIGURE 1: Location of Yuebao Open-pit Mine.

civil airport safety evaluation [29], network security risk assessment [30], and so on and achieved good results, which have provided a new idea for the research of this paper. In view of this, a dynamic variable weight model of influencing factors is proposed to analyze the dynamic change and correlation degree of slope index weight under different monthly maximum rainfall. On this basis, a dynamic evaluation model of slope stability based on UM is established to quantitatively evaluate the risk degree of slope. In addition, the method not only realizes the problem of slope stability degree analysis but also highlights the advantages in resolving the weight dynamic change of influencing factors on slope stability and the degree of correlation among the factors. It also provides technology support for the safe production and management of open-pit slope.

2. Study Area

Yuebao Open-pit Mine is located in Tanbu Town, Huadu District, Guangzhou City, China. It is about 2 kilometers away from the West Second Ring Highway on the north side and about 780 meters away from the provincial road S267. The traffic network is more developed. Its geographical coordinates are $113^{\circ}4'19''$ in the east longitude and $23^{\circ}17'50''$ in the north latitude, as shown in Figure 1. The slope in the study area is about 268.6m in length and the slope is a four-level slope with a height of each level ranging from 6.3 to 20.5m. The soil layer of the slope is mainly alluvial soft soil, peat soil, and strongly weathered argillaceous mudstone, which is subjected to underwater seepage and softening of surface fish pond for a long time. The exposed lithology on the slope is reserved for the mining area as the supporting ore body. The lithology is mainly composed of medium-micro-weathered limestone, and the rock is soft to hard. The landslide geological disaster has occurred on the HP1 slope of the mining area, as shown in Figure 2. The length of the slope is about 175m and the total inclination of the slope is about 60° . The elevation is from -73.66m to -11.40m and the height difference of rock slope is about 62.3m. The slope is about from 45° to 55° , while the top of slope is about 20° . In addition, the bedding of the rock mass is distorted by tectonic

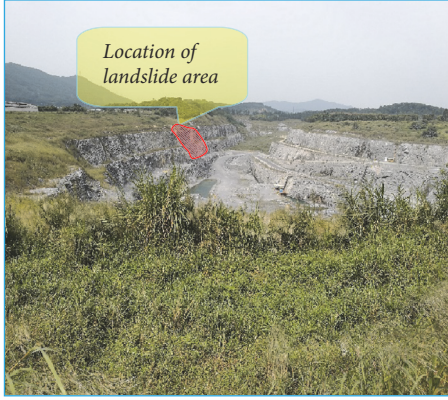


FIGURE 2: Location of landslide area.

changes, rock occurrence is $245\sim 345^\circ/55\sim 65^\circ$, and two sets of dominant joints or fractures were measured in situ. The first occurrence of JL1 is $70^\circ/35\sim 45^\circ$, and the second occurrence of JL2 is $133^\circ/85^\circ$. After cutting with the slope, it may form a wedge that is not conducive to the stability of the slope. The slope is high in the west and low in the east and is steep. In addition, the vegetation on the slope which is mainly grass and a few shrubs is not very well developed. The groundwater of the top on slope is slight seepage through the form of ascending springs, and no groundwater was exposed at the toe of slope. But there was a pool in the south side of the slope.

3. Methodology

3.1. The Construction Method of Dynamic VW. Weight is an index to measure the degree or size of slope failure affected by various factors of open-pit slope stability. The rationality and accuracy of its distribution will have a direct impact on the slope stability evaluation level. However, in the analysis and evaluation of the slope stability on open-pit mines, most researchers evaluate the weight of each index as a fixed value at home and abroad [31–33]. They rarely consider the change of the weight in influencing factors index system when it changes or takes different values, which ignore the dynamic change of slope by different index values. However, because the open-pit slope is in an open and realistic environment, the values of the factors affecting the stability are often dynamic and changing. For example, a certain factor which is the monthly maximum rainfall is set to 20mm and 200mm, respectively, when other factors are fixed and unchanged for an open-pit slope to analyze the stability state of open-pit slope. According to the actual experience and related research, it is obvious that the probability of the slope failure is much greater when the monthly maximum rainfall is 200mm. So, despite the same influencing factors, the evaluated degree and result of the slope stability are different. That is to say, the stability of open-pit slope will change with the change of the index values of influencing factors; the index weights in indicator system will also be dynamic and changing. This inevitably leads to the fact that the tradition evaluation method which is taken as the fixed values of

index weights is an uneven and unreasonable phenomenon in analyzing and evaluating the stability of open-pit slope.

In view of this, according to the references [34], it is assumed that the state vector of the influence factors in the evaluation system is $X=\{x_1, x_2, \dots, x_n\}$, which has n mappings, $w_j (j=1, 2, \dots, n)$, $[0, 1]^n \rightarrow [0, 1]$, $(x_1, x_2, \dots, x_n) \rightarrow w_j(x_1, x_2, \dots, x_n)$. And it meets the constraints:

$$\text{Normality: } \sum_{j=1}^n w_j(x_1, x_2, \dots, x_n) = 1 \quad (1)$$

Continuity: $w_j(x_1, x_2, \dots, x_n)$ ($j = 1, 2, \dots, n$) is continuous about every variable.

Monotonicity: $w_j(x_1, x_2, \dots, x_n)$ ($j = 1, 2, \dots, n$) monotonically decreases or increases with the variable x_j , then $W(x)=(w_1(X), w_2(X), \dots, w_n(X))$ is defined as a VW vector of influence factors.

In addition, suppose the mapping $S:[0, 1]^n \rightarrow [0, 1]^n$, $X \rightarrow S(X)=(S_1(X), S_2(X), \dots, S_n(X))$ is a n -dimensional penalty VW vector and meets the constraints:

$$x_i \geq x_j \implies \quad (2)$$

$$S_i(x) \leq S_j(x)$$

$S_j(X)$ is continuous for every variable, where ($j=1, 2, \dots, n$).

Then, for any constant weight vector $W=(w_1, w_2, \dots, w_n)$, there is

$$W \cdot S(X) = W(X) \cdot \sum_{j=1}^n (w_j S_j(X)) \quad (3)$$

That is,

$$W(X) = \frac{W \cdot S(X)}{\sum_{j=1}^n (w_j S_j(X))} \quad (4)$$

where $W \cdot S(X) = (w_1 S_1(X), w_2 S_2(X), \dots, w_n S_n(X))$ is the Hardarmard product.

Similarly, the limiting conditions of the incentive VW vector can be obtained. $x_i \geq x_j \implies S_i(x) \geq S_j(x)$, while the other two conditions are the same as the penalty VW vectors.

On this basis, the index data of different indicators (units) should be normalized to ensure the comparability among the influencing factors in order to calculate the dynamic weight of the indicator. There are many methods for normalization at present. In view of the different states or results of slope stability caused by various factors that present complex and dynamic changes, the normalization of slope influencing factors is usually in the following two ways [35].

One is that the value of a certain factor is larger, and the stability of the slope is better, namely, the benefit type:

$$b_{ij} = \frac{a_{ij} - \min_i(a_{ij})}{\max_i(a_{ij}) - \min_i(a_{ij})} \quad (5)$$

The other is that the value of a certain factor is smaller, and the stability state of the slope is better, namely the cost type.

$$b_{ij} = \frac{\max_i(a_{ij}) - a_{ij}}{\max_i(a_{ij}) - \min_i(a_{ij})} \quad (6)$$

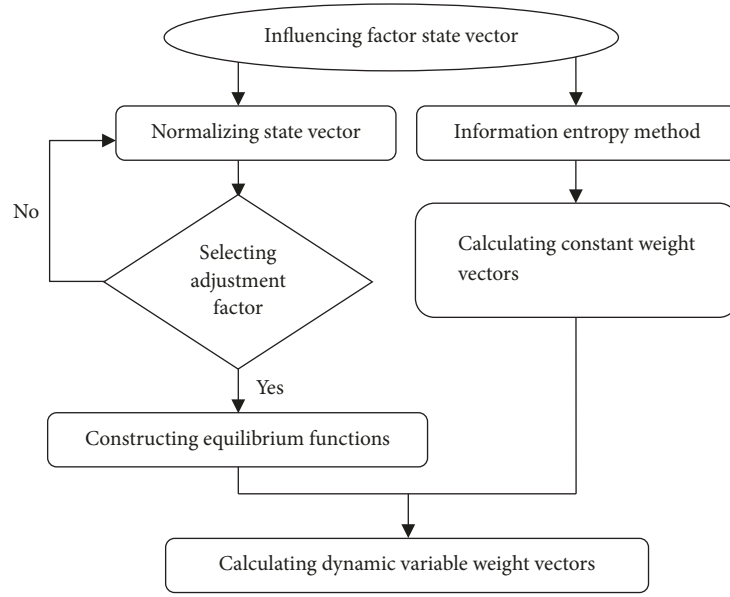


FIGURE 3: Construction process of dynamic variable weight vector.

Therefore, in the actual constructing function, the form of the equalization function can be determined first, and then the relationship between the equilibrium function and the weight change is determined according to the change of the value of each influencing factor. Finally, the equalization function is constructed by choosing the adjustment factor. The specific steps are shown in Figure 3.

3.2. *The Method of Improved VW-UM.* According to the idea of constructing the dynamic VW vector, this paper first uses the information entropy method to calculate the constant weights of each index. On the basis of this, an exponential function [36] with flexible parameter settings and strong model expansion capabilities is used to construct the VW vector by consulting the references and considering the actual conditions of the project and the construction characteristics of the equilibrium function. The specific steps and methods are as follows:

First, set w_j ($0 \leq w_j \leq 1$, $\sum_{j=1}^m w_j = 1$) as the constant weight of the j evaluation index X_j ($j=1,2,\dots,m$). According to the information entropy method, the weight of each index can be calculated by (5) and (6).

$$\nu_{ij} = 1 + \frac{1}{\lg m} \sum_{k=1}^m p_{jk} \lg p_{jk} \quad (7)$$

$$w_j = \frac{\nu_j}{\sum_{i=1}^n \nu_i} \quad (8)$$

Note that, since there is a case of $p_{jk}=0$, $\lg p_{jk}$ is meaningless in the process of entropy weight calculation. Therefore, it can be assumed that $p_{jk}=0$ when $\lg p_{jk}=0$. In addition, according to the reference [37], when the entropy value e_j becomes close to 1, the weight will be greatly different even if the entropy value changes a small amount. In view of this,

the calculation equation of the constant weight is improved as follows:

$$w_j = \frac{\exp(\sum_{t=1}^n e_t + 1 - e_j) - \exp(e_j)}{\sum_{l=1}^n [\exp(\sum_{t=1}^n e_t + 1 - e_l) - \exp(e_l)]} \quad (9)$$

Then, the VW vector function is constructed.

$$S_j(X_j) = \begin{cases} e^{\alpha(\beta-x_{ij})} & x_{ij} \leq \beta \\ 1 & x_{ij} \geq \beta \end{cases} \quad (10)$$

$$S(X) = (S_1(x_1), S_2(x_2), \dots, S_n(x_n)), \quad (11)$$

$$j = 1, 2, \dots, n; \alpha \geq 0; 0 < \beta \leq 1$$

In the above equation, β represents the negation factor of the function. If the value of the index factor x_{ij} is not greater than β , the weight value can be increased by a VW method. While α is the penalty factor of the function; that is to say, the degree of punishment will be enhanced, when the value of α increases. However, if the evaluation index factors show a relatively balanced state with each other, the comprehensive evaluation index will be larger. In practical applications, the values of α and β can be selected depending on a specific problem.

Finally, based on the calculated constant weight vector W and the constructed VW vector function $S(X)$, the VW vector matrix $W(X)$ can be calculated with (4).

4. Experimental

4.1. *Analysis of Influencing Factors.* In order to discuss and analyze the relationship among the influencing factors and construct the evaluation model, the influencing factors of slope stability should be analyzed in the study area. In general,

the main factors inducing landslide are given to the following three aspects: geological conditions, hydrological conditions, and influence of internal and external forces and human actions. In view of this, based on the investigation data of Yuebao Open-pit Mine, the main influencing factors of the slope stability in the study area are analyzed as follows.

4.1.1. Topography and Geomorphology. The mining area is located in the grounding zone of low hills and river terraces. There are many fish ponds, fruit trees, and rice fields on the ground, and the terrain is relatively flat. However, the ground of the mining area is now high in the periphery and low in the middle after mining for years. In addition, the geomorphic is more complicated in the exploration area, and the slope of which elevation is -74.59 m to 6.26 m is high in the west and low in the east. And the slope becomes steeper after mining, which provides favorable conditions for the landslide and collapse.

4.1.2. Type of Rock and Soil. According to the investigation data of the study area, the regional strata are mainly Carboniferous and Quaternary overburden whose lithology is divided into carbonaceous mudstone, carbonaceous limestone, limestone, and marl. In addition, alluvial soil and strongly weathered carbonaceous mudstone are dominant on the west side of the slope, while medium weathered limestone is dominant on the exposed surface of the slope. The stratum is strongly affected by faults, the fissures are well developed, the rock mass is very fragmented~broken, and the physical mechanics properties of rock and soil are not uniform, which will have a greater impact on the stability of the slope.

4.1.3. Geological Structure. Affected by regional folds and fault structures, there are some secondary faults which seriously affect the slope stability in the mining area and the nearby.

F2 which is about 600m and distributed on the near east side of the exploration area extends from the northwest to the southeast in the mining area. And the fault zone is northwestward, its width is about 20 m to 60m, and the length is unknown. In addition, the secondary faults (F2-1 and F2-2) are developed, and the fault scratches, distortions, and faults can be seen in the fault zone and its affected area. So, because of the indirect affection by the fault, the joint fissures of the slope rock layer are developed and variable, and the rock mass is broken.

F3 which is about 800m away from the exploration area is distributed on the northeast side of the mining area and near the east side of the exploration area. The fault is northwestward with an unknown length. The lithology in the west is the grey-white thick layered coarse sandstone of the Lower Carboniferous Zimenqiao Formation with purple-red medium-thick layered siltstone, argillaceous shale, and siliceous layer of fine sandstone. The lithology in the east is the interbedded layer of the thick layered dolomitic limestone, dolomite, and biolimestone which are grey-white, grey, and light flesh-red in the Upper Carboniferous Hutian Group. But the faults have little impact on the exploration area.

F10 which is about 550m away from the exploration area is distributed on the north side of the exploration area. And it is presumed to be a small secondary fault caused by the northeast anticline, which is oriented to the near eastward with a length of about 260m. Because of the fracture, the limestone of the Lower Carboniferous Shidengzi Group has fault which is a compression-torsion fracture.

F11 which is about 650m away from the exploration area is distributed on the north side of the exploration area. And it is presumed to be a small secondary fault caused by the northeast anticline, which is oriented to the near northwestward with a length of about 360m. Because of the fracture, the limestone of the Lower Carboniferous Shidengzi Group has fault which is a compression-torsion fracture.

F13 which is northwestward with a length of about 230m is distributed in the exploration area. The lithology on the west is the sandstone, siltstone, and sandy shale which are interbedded with sandstone conglomerate, argillaceous shale, carbonaceous shale, multilayer inferior coal seams of the Lower Carboniferous Ceshui Formation, and the medium-thick layered limestone, breccia limestone, dolomitic limestone in the fourth member of the Lower Carboniferous Shidengzi Group. The lithology on the east is the medium-thick layered limestone, breccia limestone, and dolomitic limestone in the fourth member of the Lower Carboniferous Shidengzi Group. The slope is located on the eastern side of the fault that has a great influence on the exploration area. The scratches, rock distortion, faults, and fault breccias can be seen in the affected area of faults, which results in the developed joint fissures, the changeable occurrence, and the broken rock of the slope. So, the fracture of rock mass is an important reason that affects the stability and causes landslides of the slope.

4.1.4. Hydrology. There are mainly surface water and groundwater. The surface water is dominated by fish ponds and the bottom pool of the pit. The fish ponds are distributed on the west side of soil road on the controlled slope top, the closest distance to the perimeter of the landslide is about 48m, and the water level elevation of the fish pond is about 2.89m during the exploration period. The pool is closely related to the groundwater and has an important impact on the stability of the slope. So, due to the influence of the fish pond water, the surface water is infiltrated into the pit. But owing to the relative water-blocking effect of the limestone ore body on the edge of the pit, the infiltrated surface water is failed to be completely discharged through the karst fissure, and part of the surface water slightly seeps in the form of ascending spring on the top of the landslide area. The collecting pool of the pit which is distributed at the foot of the east slope is a component of the drainage system in the mining area. The water level is about 30cm lower than the periphery of the pit, and the elevation is about -72.3m. So, the drainage system has less impact on the groundwater in the exploration area. However, the groundwater is mainly recharged by surface runoff and seepage through fishpond water and atmospheric rainfall and exists in the form of pore groundwater in soil layer and karst fissure water in bedrock. The surface water generated by rainfall forms instantaneous

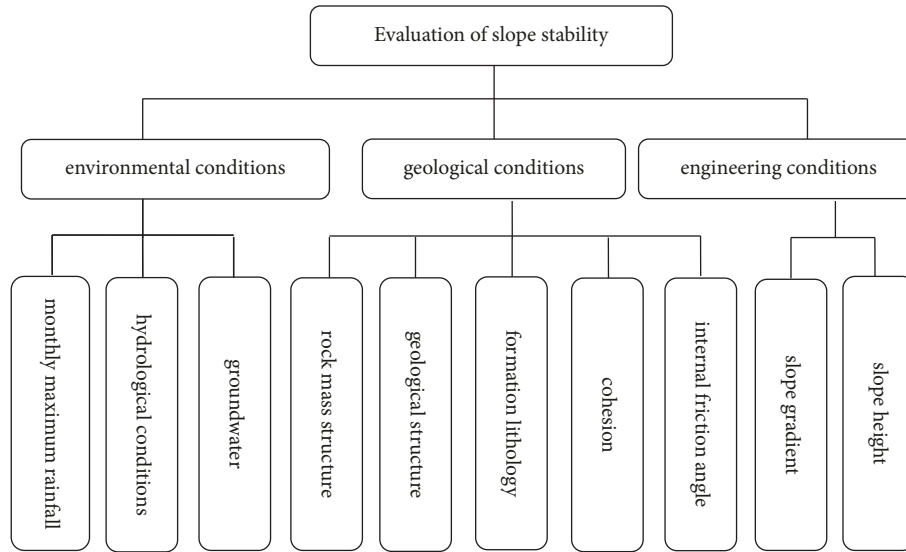


FIGURE 4: Evaluation factors of slope stability in Yuebao Open-pit Mine.

sheet runoff, which partly seeps into the underground, and the surface runoff disappears quickly until the rainfall is over. Moreover, groundwater flows into the drainage system of the pit; an amount seeps into karst fissures and some evaporates. However, the karst fissure water is unevenly enriched in the karst fissures due to the obvious traces of karst erosion in the study area and the strong influence of the rock tectonic. So, the groundwater belongs to category A.

4.1.5. Influence of Internal and External Forces and Human Actions. The basic intensity of earthquake resistance in mining area is 6 degrees, which can basically meet the safety production of mining area. The external force has relatively little impact on the slope, and the main factors influencing the collapse and landslide are rainfall and unreasonable human activities (such as excavation foot of slope).

4.2. Extraction of Influencing Factors. On the basis of the analysis of the above-mentioned influencing factors, after the field investigation and consultation with the experts of the geology chief engineer and the project leader, it is agreed that the main factors affecting the stability of the open-pit slope are geological conditions: rock mass structure (X_1), geological structure (X_2), formation lithology (X_3), internal friction angle (X_4), cohesion (X_5); environmental conditions: groundwater (X_6), hydrological condition (X_7), monthly maximum rainfall (X_8); and engineering conditions: slope gradient (X_9) and slope height (X_{10}), as shown in Figure 4.

4.3. Establishment of Evaluation Index System. In order to more clearly reflect the influence of each index on slope stability and the risk degree of slope, we set the risk assessment level of the Yuebao Open-pit Mine slope as $\{C_1, C_2, C_3, C_4\}$, namely, Grade I, Grade II, Grade III, Grade IV, which indicate the extremely high risk, the high risk, the general risk, and the low risk, respectively. In addition, it can be seen that

these indicators are qualitative and quantitative based on the analysis of the above 10 influencing factors. To clearly express the relationship between each index factor and the slope stability grade, we classified and assigned five qualitative factors such as rock mass structure, geological structure, formation lithology, groundwater, and hydrological condition, as shown in Table 2. Besides, we graded and evaluated the five quantitative factors such as internal friction angle, cohesion, slope height, slope gradient, and monthly maximum rainfall and established an evaluation index system, as shown in Table 3.

4.4. Establishment of Dynamic Evaluation Model. To scientifically and accurately evaluate the stability and risk degree of the Yuebao Open-pit Mine slope, this paper has established an evaluation model based on the modeling thought of reference [25].

According to the data of geology, hydrology, and environment collected from the slope of open-pit mine, we can see that rock mass of HP1 slope is broken; its joint fissure is developed; the formation lithology is mainly composed of shale and sandstone; the groundwater is slightly exuded through the form of ascending springs; surface water is permeable and has weak interlayer. Therefore, according to the basic principles of qualitative index assignment and the experimental data of rock parameters in Table 2, 10 qualitative and quantitative index data values of HP1 slope under different monthly maximum rainfall conditions are listed in Table 4. Special attention is given to that the value of each index of the slope should be assigned according to the actual reference value under the condition of monthly maximum rainfall.

So, according to the single index measurement function and the evaluation matrix construction method, the single index measurement function of the influencing factors of HP1 slope was shown in Figures 5(a)–5(f).

TABLE 2: Qualitative index system for risk assessment of slope in Yuebao Open-pit Mine and the corresponding evaluation grade and assignment.

Classification of influence degree	Assignment	Influencing factor				
		Rock mass structure (X_1)	Geological structure (X_2)	Formation lithology (X_3)	Ground-Water (X_6)	Hydrological condition (X_7)
Grade I (C_1)	1	The rock mass is soft and broken, and its structural plane is developed	Fault joints and fractures are very developed, and the rock mass is broken approximately	soft rock	medium water pressure	strong permeability and weak surface
Grade II (C_2)	2	The rock mass is relatively soft and broken, and the structural plane is relatively developed	There are faults, fractures are developed, and the integrity of rock mass is poor	soft rock~a little hard	fissure water	medium permeable and weak interlayer
Grade III (C_3)	3	The rock mass is relatively complete with layered structure	There are faults, fractures are developed, and rock mass integrity is medium	a little hard	moist	weak water permeability and weak interlayer affecting engineering quality
Grade IV (C_4)	4	The rock mass is massive lump	No fault or small fault that does not affect the project, slightly developed fracture	hard	dry	water permeability is small, no weak side

TABLE 3: Quantitative index system for risk assessment of slope in Yuebao Open-pit Mine and the corresponding evaluation criteria.

Classification of influence degree	Influencing factor				
	Internal friction angle (X_4)	Cohesion (X_5)	Monthly maximum rainfall (X_8)	Slope gradient (X_9)	Slope height (X_{10})
Grade I (C_1)	<18	<0.05	>300	60~80	>100
Grade II (C_2)	27~18	0.09~0.05	150~300	40~60	60~100
Grade III (C_3)	35~27	0.13~0.09	80~150	20~40	20~60
Grade IV (C_4)	>35	>0.13	<80	0~20	<20

TABLE 4: Risk assessment index value of different factors in HP1 slope under different months of maximum rainfall.

Program	X_1	X_2	X_3	X_4 ($^{\circ}$)	X_5 Mpa	X_6	X_7	X_8 mm	X_9 ($^{\circ}$)	X_{10} m
S_1	2	2	2	26	0.1	3	3	60	50	79.6
S_2	2	2	2	21	0.06	2	2	120	50	79.6
S_3	2	2	2	21	0.06	2	2	240	50	79.6
S_4	2	2	2	21	0.06	2	2	300	50	79.6

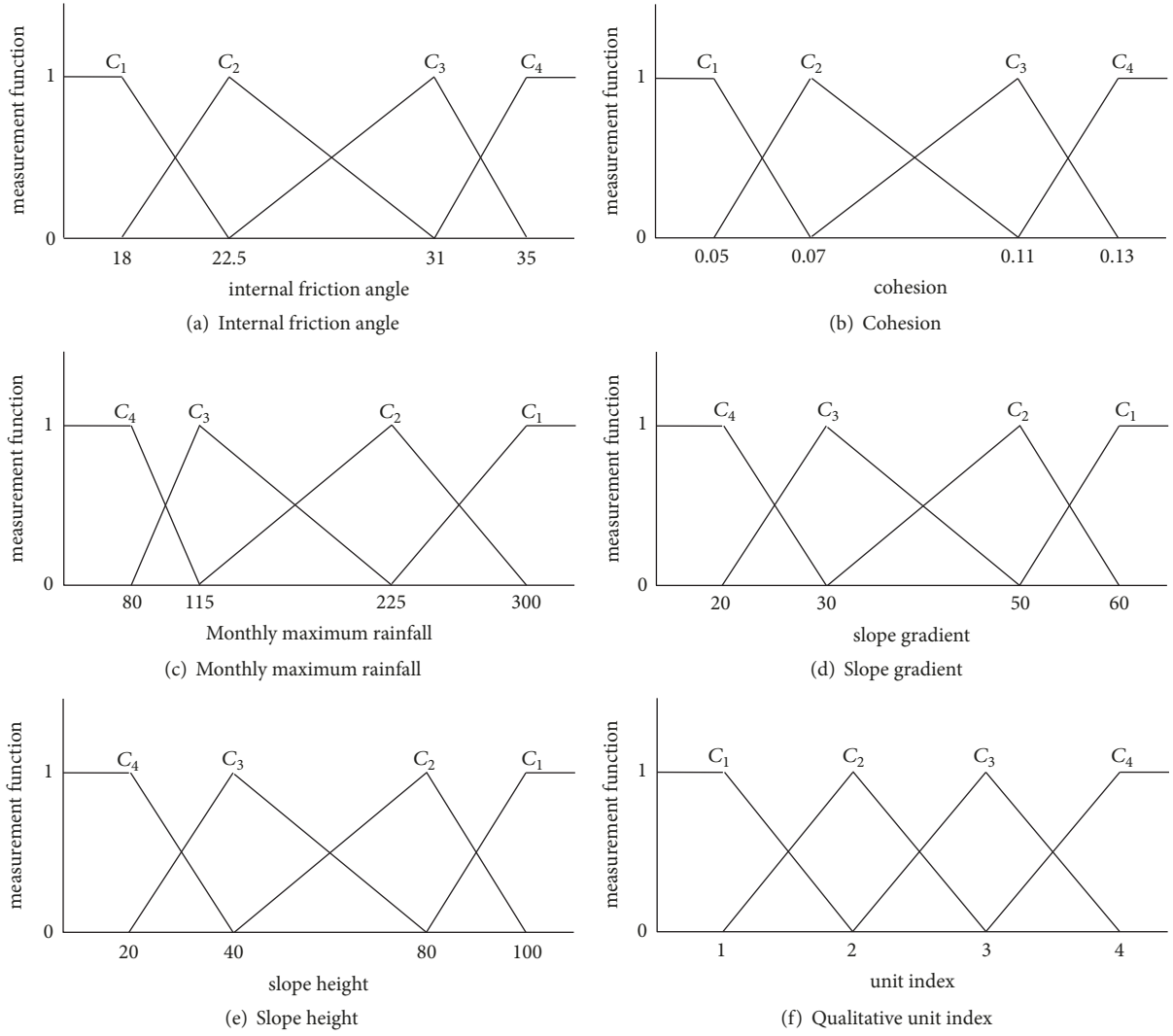


FIGURE 5: The single index measure function of the influencing factors of the HP_1 slope.

Therefore, the single index evaluation matrix of the HPI slope was calculated as follows:

$$(\mu_{1jk})_{10 \times 4} = \begin{bmatrix} 0 & 1 & 0 & 0 \\ 0 & 1 & 0 & 0 \\ 0 & 1 & 0 & 0 \\ 0 & 0.5882 & 0.4118 & 0 \\ 0 & 0.25 & 0.75 & 0 \\ 0 & 0 & 1 & 0 \\ 0 & 0 & 1 & 0 \\ 0 & 0 & 0 & 1 \\ 0 & 1 & 0 & 0 \\ 0 & 0.99 & 0.01 & 0 \end{bmatrix} \quad (12)$$

Similarly, the single index evaluation matrix $(\mu_{2jk})_{10 \times 4}$, $(\mu_{3jk})_{10 \times 4}$, $(\mu_{4jk})_{10 \times 4}$ of the HPI slope could be obtained separately in the other three cases.

5. Results and Discussion

5.1. Results. According to the above calculation method, the normalized index matrix B was calculated first. Then, according to the analysis of the value of normalized index matrix B and the actual situation of the slope, the α value was set to 0.5 and the negative parameter β value was set to 0.3. Finally, the index constant weight vector w , the VW vector W , and the multi-index measure vector μ of the HPI slope under different monthly maximum rainfall conditions were calculated, respectively, as follows:

$$[w] = [0.0903 \ 0.0903 \ 0.0903 \ 0.0980 \ 0.1132 \ 0.0939 \ 0.1224 \ 0.1206 \ 0.0903 \ 0.0903]$$

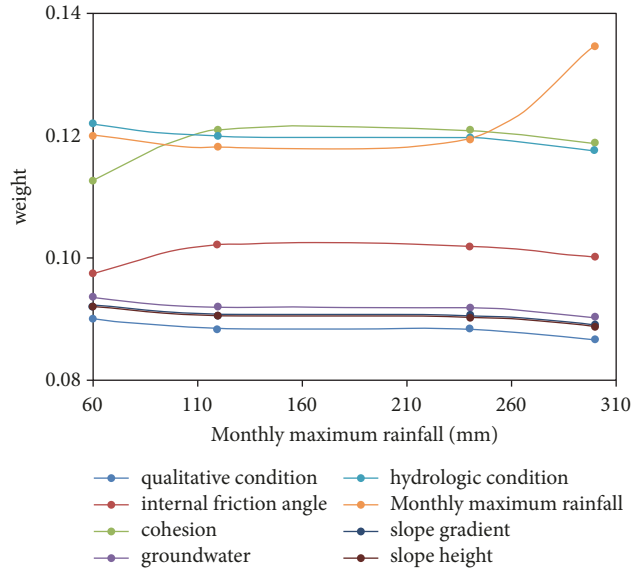


FIGURE 6: Weight change of the slope influence factors with the monthly maximum rainfall.

$$[B] = \begin{bmatrix} 0.3333 & 0.3333 & 0.3333 & 0.4706 & 0.6250 & 0.6667 & 0.6667 & 1 & 0.25 & 0.255 \\ 0.3333 & 0.3333 & 0.3333 & 0.1765 & 0.1250 & 0.3333 & 0.3333 & 0.8182 & 0.25 & 0.255 \\ 0.3333 & 0.3333 & 0.3333 & 0.1765 & 0.1250 & 0.3333 & 0.3333 & 0.2727 & 0.25 & 0.255 \\ 0.3333 & 0.3333 & 0.3333 & 0.1765 & 0.1765 & 0.3333 & 0.3333 & 0 & 0.25 & 0.255 \end{bmatrix}$$

$$[W] = \begin{bmatrix} 0.0900 & 0.0900 & 0.0900 & 0.0976 & 0.1127 & 0.0935 & 0.1219 & 0.1201 & 0.0922 & 0.0920 \\ 0.0885 & 0.0885 & 0.0885 & 0.1022 & 0.1210 & 0.0920 & 0.1199 & 0.1182 & 0.0907 & 0.0905 \\ 0.0884 & 0.0884 & 0.0884 & 0.1020 & 0.1208 & 0.0919 & 0.1197 & 0.1196 & 0.0906 & 0.0904 \\ 0.0868 & 0.0868 & 0.0868 & 0.1002 & 0.1188 & 0.0903 & 0.1176 & 0.1347 & 0.0890 & 0.0888 \end{bmatrix}$$

$$[\mu] = \begin{bmatrix} 0 & 0.5388 & 0.3411 & 0.1201 \\ 0.0946 & 0.7917 & 0.1137 & 0 \\ 0.1183 & 0.8808 & 0.0009 & 0 \\ 0.2275 & 0.7716 & 0.0009 & 0 \end{bmatrix}$$

(13)

Therefore, the change of the weight of each influencing factor of HP1 slope under different monthly maximum rainfall conditions was obtained as shown in Figure 6.

In addition, referring to the above of the slope stability confidence level $\lambda=0.6$, by (13) it can be concluded that the risk degrees of HP1 slope under different monthly maximum rainfall conditions are Grade III (general risk), Grade II (high risk), Grade II (high risk), and Grade II (high risk).

The results of Figure 6 show that the weight of monthly maximum rainfall and the risk degree of slope increase accordingly with the increase of rainfall. Mine management departments should pay attention to the prevention and control of HP1 slope in the case of continuous rainfall. Then in practice, according to the measured data of the mining area, the HP1 slope affected by geological environmental

conditions, mining excavation, water seepage in the western fish pond, and natural factors has caused geological disasters like landslide under continuous heavy rainfall conditions since October 2016, which has a high degree of agreement with the model prediction results. It can be seen that the risk assessment and the prediction stability of the slope have strong reliability by using the improved dynamic VW-UM, which can guide the safe production and prevention in mining area.

In addition, the factors affecting the stability of HP1 slope are characterized by irregularity, nonlinearity, and strong coupling. In this paper, according to the above-mentioned risk classification principle of slope, we have sorted $C_1 > C_2 > C_3 > C_4$ to more intuitively and clearly reflect the relationship between the index weights of HP1 slope, and the values are

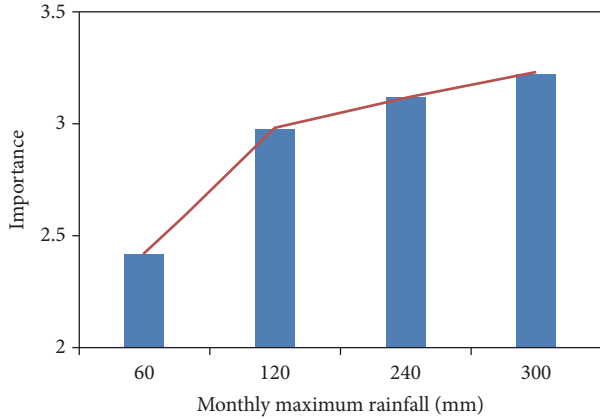


FIGURE 7: The trend of risk degree of HP_1 slope.

respectively assigned as $I_1=4, I_2=3, I_3=2, I_4=1$ to facilitate the calculation and quantitatively determine the risk degree of slope. The method of calculating the relative Rq is proposed to quantitatively analyze the slope stability and the change trend of index weight of HP_1 slope under different monthly maximum rainfall conditions, which can be calculated as shown in

$$q_{S_i} = \sum_{l=1}^p I_l \mu_{li} \quad (14)$$

Therefore, according to the above-mentioned assignment and risk calculation methods, the RI of the HP_1 slope in the four cases was calculated as follows:

$$\begin{aligned} q_{S_1} &= 2.4187 \\ q_{S_2} &= 2.9809 \\ q_{S_3} &= 3.1174 \\ q_{S_4} &= 3.2266 \end{aligned} \quad (15)$$

That is,

$$q_{S_4} > q_{S_3} > q_{S_2} > q_{S_1} \quad (16)$$

The trend of the RI of the HP_1 slope under different monthly maximum rainfall conditions was shown in Figure 7.

5.2. Discussion. (1) With the increase of monthly maximum rainfall, HP_1 slope stability decreases gradually, and its risk level increased from Grade III to Grade II; that is, the risk degree of landslide on HP_1 slope increased from general to high, and the slope may be unstable. And according to the measured data in the mining area, since October 2016, the HP_1 slope has landslides under the continuous heavy rainfall, which has verified the feasibility of the dynamic variable weight evaluation model.

(2) According to the index value of RI q , the q varies greatly which indicates the slope stability changes obviously

in the early stage of rainfall when the monthly maximum rainfall increases from 60 mm to 120 mm, and the risk level increases from general to high. When the monthly maximum rainfall is 120 mm, 240 mm, and 300 mm, respectively, although the risk level of the slope has not changed, the q increases gradually, which indicates that the instability of the slope increases gradually when the monthly maximum rainfall reaches a certain level and eventually leads to geological disasters like landslides for HP_1 slope.

(3) Among the four research schemes, although the evaluation indexes affecting slope stability have not changed, it can be seen from Figure 6 that the weight of each index changes with the change of the maximum monthly rainfall, and its weight is no longer a fixed value but presents a nonlinear and dynamic change law.

(4) When the monthly maximum rainfall increases from 60 to 120 mm, its weight decreases, while the weight of internal friction angle and cohesion increases. The weight of internal friction angle and cohesion decreases gradually when the monthly maximum rainfall increases from 120 mm to 300 mm, while the weight of monthly maximum rainfall increases gradually and reaches the maximum and is the largest in all. It can be seen that the slope stability is a comprehensive reflection of the interaction on influencing factors and also fully reflects the characteristics of coupling among the influencing factors, especially the strong correlation among the monthly maximum rainfall, internal friction angle, and cohesion.

(5) Although the research results in this paper have solved the dynamic change of the influencing factors weight and the dynamic evaluation of the slope risk degree. There is certain one-sidedness in the selection of influencing factors which is mainly based on field investigation and expert experience. In addition, the method fails to reveal the deformation mechanism of the slope. So, compared with the similar material model, numerical simulation, and other stability evaluation methods mentioned above, it has still some shortcomings. In view of this, the authors will use the similar material and numerical model to excavate the main influencing factors of slope in the future research in order to more accurately evaluate the risk level of slope and improve the accuracy of model prediction.

6. Conclusions

(1) In order to overcome the shortcomings of the fixed weight on influencing factors in previous slope stability studies, a dynamic variable weight model of influencing factors was constructed, and the weights of each index were calculated under different monthly maximum rainfall. The results show that the weight of each index on slope stability influencing factors is no longer a fixed value but presents a nonlinear and dynamic change law under different monthly maximum rainfall, and there is a strong correlation among the maximum rainfall, internal friction angle, and cohesion.

(2) The dynamic variable weight risk evaluation model of slope based on unascertained measurement is constructed, and the stability state of slope is analyzed under different monthly maximum rainfall. The research shows that the risk degree of slope varies with the change of monthly maximum

rainfall, and the evaluation results are in good agreement with the actual situation of HPI slope and have verified the feasibility of the model. The stability of open-pit slope does not change with the change of influencing factors. In addition, the RI index q is put forward to quantitatively evaluate the risk degree of slope. The results show that the value of q increases and the risk degree of slope increases gradually with the increase of monthly maximum rainfall.

(3) Rainfall is an important factor affecting slope landslides. Slope stability changes dynamically with different rainfall, and its risk level (degree) is also changing constantly. The paper carries out dynamic evaluation and analysis of slope stability under different rainfall. The results have important guiding significance for the study of the stability analysis on open-pit slope and related fields and can provide important technical support for the safe production and management of mines.

Data Availability

The data used to support the findings of this study are available from the corresponding author upon request.

Conflicts of Interest

The authors declare that they have no conflicts of interest.

Acknowledgments

This work was supported by the Education Department of Jiangxi Province (No. GJJ161570 and No. GJJ170524) and the NASS Key Laboratory of Land Environment and Disaster Monitoring (No. LEDM2018B01).

References

- [1] J. H. Wen, Y. Y. Zhang et al., "Research status of instability mechanism of rainfall-induced landslide and stability evaluation model," *China Journal of Highway and Transport*, vol. 31, no. 2, 2018.
- [2] D. Liu, E. Wang, J. Song, and C. Zhang, "The relation between landslide and rainfall and prediction method of western open-pit coal mine of Fushun," *Journal of Catastrophology*, pp. 50–54, 2008.
- [3] B.-G. Chae, H.-J. Park, F. Catani, A. Simoni, and M. Berti, "Landslide prediction, monitoring and early warning: a concise review of state-of-the-art," *Geosciences Journal*, vol. 21, no. 6, pp. 1033–1070, 2017.
- [4] J. Ding, Z. Yang, Y. Shang, S. Zhou, and J. Yin, "A new method for spatio-temporal prediction of rainfall-induced landslide," *Science China Earth Sciences*, vol. 49, no. 4, pp. 421–430, 2006.
- [5] F. C. Dai, C. F. Lee, and S. J. Wang, "Characterization of rainfall-induced landslides," *International Journal of Remote Sensing*, vol. 24, no. 23, pp. 4817–4834, 2003.
- [6] B. D. Collins and D. Znidarcic, "Stability analyses of rainfall induced landslides," *Journal of Geotechnical and Geoenvironmental Engineering*, vol. 130, no. 4, pp. 362–372, 2004.
- [7] E. Conte, A. Donato, and A. Troncone, "A simplified method for predicting rainfall-induced mobility of active landslides," *Landslides*, vol. 14, no. 1, pp. 35–45, 2017.
- [8] E. Conte, A. Donato, L. Pugliese, and A. Troncone, "Analysis of the Maierato landslide (Calabria, Southern Italy)," *Landslides*, vol. 15, no. 10, pp. 1935–1950, 2018.
- [9] E. Conte and A. Troncone, "A performance-based method for the design of drainage trenches used to stabilize slopes," *Engineering Geology*, vol. 239, pp. 158–166, 2018.
- [10] M. Ji, W. Li, T. Guo, and Z. Yang, "Model experimental study on the relationship between landslide and rainfall," *Journal of Railway Science and Engineering*, vol. 14, no. 12, pp. 2586–2593, 2017.
- [11] C.-C. Lin and C.-M. Lo, "Investigation of rainfall-induced failure processes and characteristics of cataclinal and anaclinal slopes using physical models," *Environmental Earth Sciences*, vol. 77, no. 5, p. 210, 2018.
- [12] C. Li, D. Yao, Z. Wang et al., "Model test on rainfall-induced loess–mudstone interfacial landslides in Qingshuihe, China," *Environmental Earth Sciences*, vol. 75, no. 9, pp. 1–18, 2016.
- [13] Z. Li, Y. J. He, H. Li, and H. Xu, "Model test on slope landslides under antecedent rainfall," *Journal of Hohai University (Natural Sciences)*, vol. 44, no. 5, pp. 400–405, 2016.
- [14] H. Dong, Z. Li, X. Jiang, and C. Qu, "Model test research on the gravel-cluttered soil slope under the heavy artificial rainfall condition," *Journal of Safety and Environment*, vol. 16, no. 4, pp. 236–241, 2016.
- [15] M. Suradi, A. B. Fourie, and M. J. Saynor, "An experimental and numerical study of a landslide triggered by an extreme rainfall event in northern Australia," *Landslides*, vol. 13, no. 5, pp. 1125–1138, 2016.
- [16] C.-M. Lo, C.-F. Lee, and W.-K. Huang, "Failure mechanism analysis of rainfall-induced landslide at Pingguang stream in Taiwan: mapping, investigation, and numerical simulation," *Environmental Earth Sciences*, vol. 75, no. 21, p. 1422, 2016.
- [17] Y. H. He, "Numerical simulation on dump slope stability under rainfall infiltration," *Journal of Yangtze River Scientific Research Institute*, vol. 32, no. 2, pp. 44–47, 2015.
- [18] K. Zhao, L. X. Yu et al., "Research on rock slope stability in the condition of rainfall or blasting vibration," *Journal of Jiangxi University of Science and Technology*, pp. 43–48, 2015.
- [19] X. J. Yang, D. G. Hou, Z. Hao, Z. Tao, H. Shi, and K. Jin, "Research on correlations between slope stability and rainfall of high steep slope on Nanfen open-pit iron ore," *Chinese Journal of Rock Mechanics and Engineering*, vol. 35, pp. 3232–3240, 2016.
- [20] Y. L. Li, B. Chen, C. Ma, and B. Zhou, "Study on the stability of the foundation pit slope under rainfall infiltration conditions based on ABAQUS," *Chinese Journal of Applied Mechanics*, vol. 34, no. 1, pp. 155–161, 2017.
- [21] N. Saadatkhah, A. Kassim, L. M. Lee, and J. Rahnamarad, "Spatiotemporal regional modeling of rainfall-induced slope failure in Hulu Kelang, Malaysia," *Environmental Earth Sciences*, vol. 73, no. 12, pp. 8425–8441, 2015.
- [22] N. Saadatkhah, A. Kassim, and L. M. Lee, "Hulu Kelang, Malaysia regional mapping of rainfall-induced landslides using TRIGRS model," *Arabian Journal of Geosciences*, vol. 8, no. 5, pp. 3183–3194, 2015.
- [23] Y. Mao, Z. Zhou, Z. Peng, and X. Gao, "Landslide hazard prediction based on uncertain multi-classification support vector machine method," *Journal of Jiangxi University of Science and Technology*, vol. 37, no. 3, pp. 102–108, 2016.
- [24] S.-W. Shen, L. Nai, and Y. Xu, "Two-stage fuzzy comprehensive evaluation for rainfall influence on slope stability under different weight value," *Journal of Jilin University (Earth Science Edition)*, vol. 42, no. 3, pp. 777–784, 2012.

- [25] H.-P. Xiao, G.-L. Guo, and W. Liu, "Hazard degree identification and coupling analysis of the influencing factors on goafs," *Arabian Journal of Geosciences*, vol. 10, no. 3, p. 68, 2017.
- [26] T. T. Luan, Z. H. Xie, Z. Wu, N. He, and X. Zhang, "Risk evaluation model of waste dump landslide based on uncertainty measurement theory," *Journal of Central South University (Science and Technology)*, vol. 45, no. 5, pp. 1612–1617, 2014.
- [27] W. Wang, J. Li, J. Wang, Q. Fu, and W. Kang, "Highway traffic efficiency evaluation based on unascertained measure model," *Journal of Zhejiang University (Engineering Science)*, vol. 50, no. 1, pp. 48–54, 2016.
- [28] A.-H. Liu, L. Dong, and L.-J. Dong, "Optimization model of unascertained measurement for underground mining method selection and its application," *Journal of Central South University of Technology*, vol. 17, no. 4, pp. 744–749, 2010.
- [29] J. N. Zhao, L. N. Shi, and L. Zhang, "Application of improved unascertained mathematical model in security evaluation of civil airport," *International Journal of System Assurance Engineering & Management*, vol. 8, no. 3, pp. 1–12, 2017.
- [30] J. L. Chen, "A network security risk assessment model based on unascertained mathematics," *Journal of Air Force Engineering University (Natural Science Edition)*, vol. 15, no. 2, pp. 91–94, 2014.
- [31] D. Huang, X. Shi, X. Qiu, and Y. Gou, "Stability gradation of rock slopes based on multilevel uncertainty measure-set pair analysis theory," *Journal of Central South University (Science and Technology)*, vol. 48, no. 4, pp. 1057–1064, 2017.
- [32] X. Wang, Q. Kang, J. Qin, Q. Zhang, and S. Wang, "Application of AHP-extenics model to safety evaluation of rock slope stability," *Journal of Central South University (Science and Technology)*, vol. 44, no. 6, pp. 2455–2462, 2013.
- [33] Y. P. Zhu and H. H. Mo, "Application of gray correlation analysis to rock slope stability estimation," *Chinese Journal of Rock Mechanics and Engineering*, vol. 23, no. 6, pp. 915–919, 2004.
- [34] X. Wang, T. Li, Q. Chen, W. Yang, and H. Li, "Filling way optimization based on VW theory and TOPSIS," *Journal of Central South University (Science and Technology)*, pp. 198–203, 2016.
- [35] J. Shao and Y. J. Huang, "Risk assessment on ecosystem in Western underdeveloped region based on VWing-uncertainty measurement theory," *Journal of Xi'an University of Finance and Economics*, vol. 30, no. 5, pp. 26–33, 2017.
- [36] Q. Kang, X. Wang M et al., "Application of VW-UM model in stope stability evaluation," *China Safety Science Journal*, vol. 25, no. 7, pp. 128–134, 2015.
- [37] Q. Yang, "Safety evaluation of slope stability based on coefficient method and its application," *Yellow River*, vol. 38, no. 4, pp. 109–112, 2016.

